REPORT | HIV

Platelets from HIV-infected individuals on antiretroviral drug therapy with poor CD4$^+$ T cell recovery can harbor replication-competent HIV despite viral suppression

Fernando Real[1,2,3], Claude Capron[4], Alexis Sennepin[1,2,3], Riccardo Arrigucci[5], Aiwei Zhu[1,2,3], Gérémy Sannier[1,2,3], Jonathan Zheng[1,2,3], Lin Xu[1,2,3], Jean-Marc Massé[2,3,6], Ségolène …
+ See all authors and affiliations

Science Translational Medicine 18 Mar 2020:
Vol. 12, Issue 535, eaat6263
DOI: 10.1126/scitranslmed.aat6263

Hidden in plain sight

Human platelets carry out several immune functions as well as hemostasis and interact with infectious pathogens including HIV in vitro. Real *et al*. now report that platelets from HIV-infected individuals can harbor replication-competent HIV, despite successful viral suppression by antiretroviral drug therapy (ART). Moreover, in their study, >80% of virally suppressed HIV-infected individuals with platelets containing HIV showed poor restoration of immune status even 1 year after ART treatment initiation. Platelets carrying HIV may provide an alternative pathway for HIV dissemination in HIV-infected individuals on ART with viral suppression and poor CD4$^+$ T cell recovery.

Abstract

In addition to hemostasis, human platelets have several immune functions and interact with infectious pathogens including HIV in vitro. Here, we report that platelets from HIV-infected individuals on combined antiretroviral drug therapy (ART) with low blood CD4$^+$ T cell counts (<350 cells/μl) contained replication-competent HIV despite viral suppression. In vitro, human platelets harboring HIV propagated the virus to macrophages, a process that could be prevented with the biologic abciximab, an anti–integrin αIIb/β3 Fab. Furthermore, in our cohort, 88% of HIV-infected individuals on ART with viral suppression and with platelets containing HIV were poor immunological responders with CD4$^+$ T cell counts remaining below <350 cells/μl for more than one year. Our study suggests that platelets may be transient carriers of HIV and may provide an alternative pathway for HIV dissemination in HIV-infected individuals on ART with viral suppression and poor CD4$^+$ T cell recovery.

INTRODUCTION

investigation of replication-competent virions in human platelets (*12*, *13*) and in megakaryocytes (*14*) from untreated HIV-infected individuals. However, evidence for platelets containing infectious HIV in vivo, especially in HIV-infected individuals on combined antiretroviral drug therapy (ART), remains elusive.

Here, we investigated the occurrence of replication-competent HIV in platelets from HIV-infected individuals on ART with viral suppression and analyzed whether a correlation existed with their clinical status.

RESULTS

Platelets from HIV-infected individuals on ART harbor HIV

We isolated platelets from HIV-infected individuals on ART (tables S1 and S2), who had either a detectable viral load (n = 15) or undetectable virus (n = 27) that was below the limit of detection (LOD) of 1.6 $\log_{10}$ HIV RNA copies/ml, and we used quantitative real-time polymerase chain reaction (qPCR) to establish whether the isolated platelets contained HIV. In a subgroup of ART-treated HIV-infected individuals with undetectable blood viral load (10 of 27), platelets were found to contain on average 9.92 HIV RNA copies per million platelets with a confidence interval (CI) of 6.5 to 17.8 (**Fig. 1A**). A subgroup of ART-treated HIV-infected individuals with detectable viremia (10 of 15) had on average 122.3 HIV RNA copies per million platelets (CI, 65 to 1111) (**Fig. 1A**). Longitudinal clinical data obtained from these HIV-infected individuals on ART with undetectable viral load at the date of sampling (indicated by an asterisk in table S3) showed that the viral load for six of nine individuals consistently remained below the LOD for more than 1 year (median, 26 months; CI, 14 to 74 months) before the date of sampling (table S3). This finding suggested that circulating HIV had not attached nonspecifically to platelets in the circulation. Furthermore, potential contamination by HIV-infected cells present in the blood of these individuals was evaluated by flow cytometry. Analyses of platelet-rich plasma samples from all assessed HIV-infected individuals on ART detected less than one lymphocyte per sample corresponding to 2.16 $CD3^+$ T cells per million platelets (CI, 1.4 to 2.7) (fig. S1, A to C). The likelihood of platelet contamination by HIV-infected T cells was low given that in HIV-infected individuals on ART with undetectable viral load, HIV-infected T cells represented 0.01 to 0.1% of total blood $CD4^+$ T cells with 100 to 1000 HIV DNA copies per million $CD4^+$ T cells (*15*).

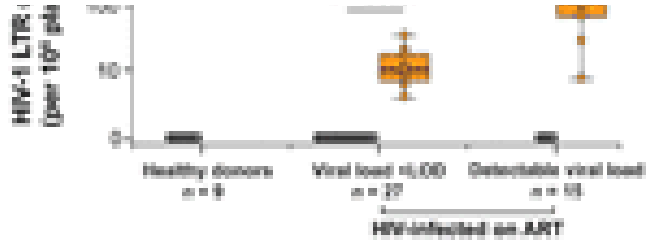

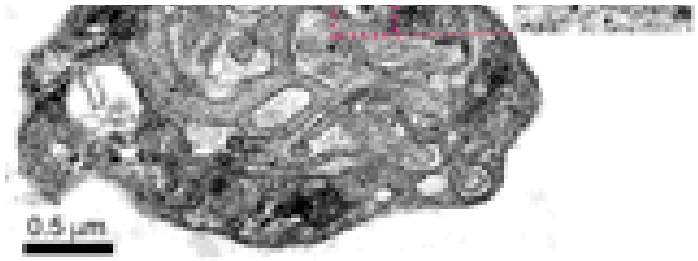

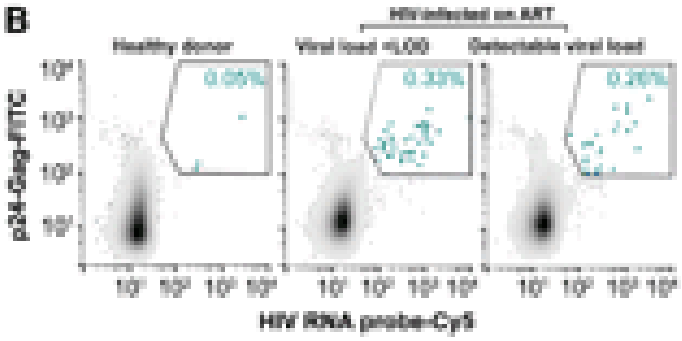

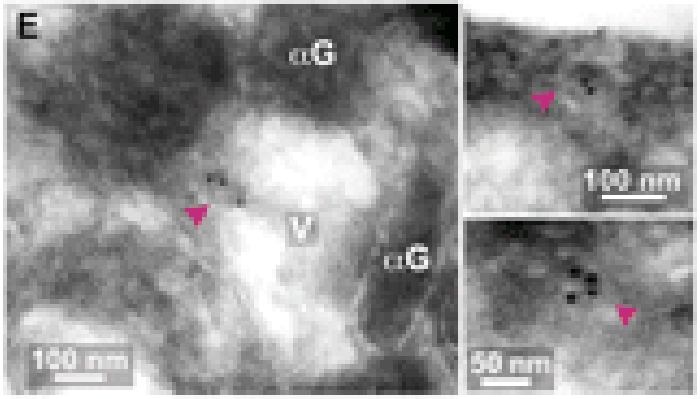

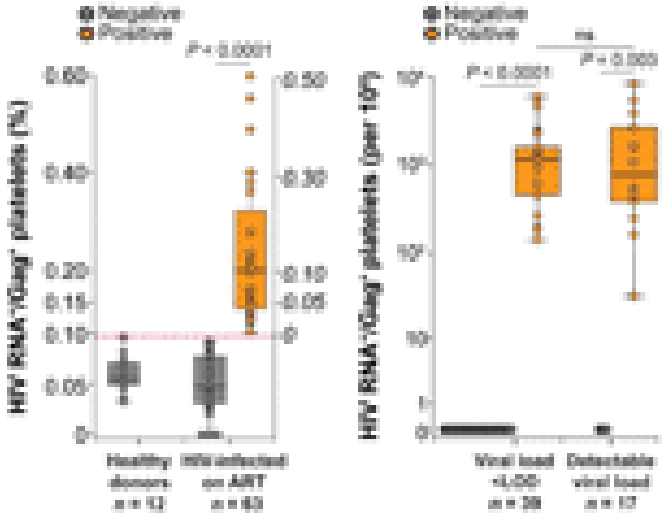

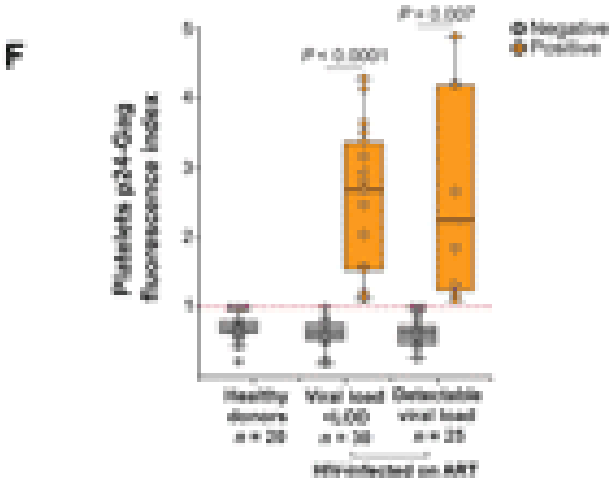

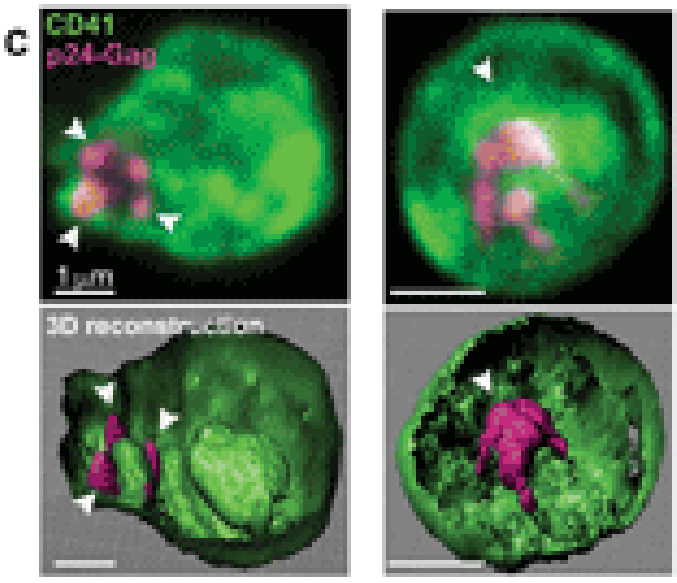

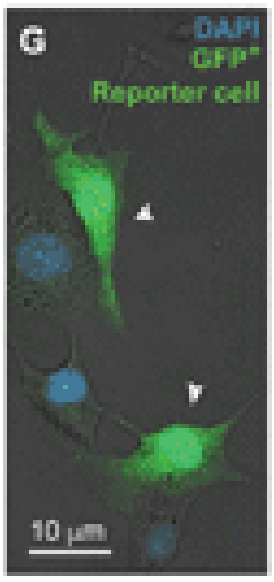

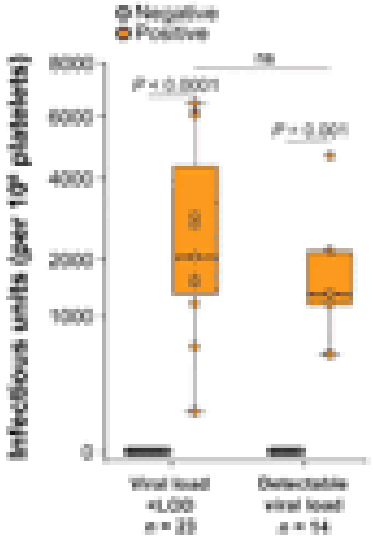

Top: HIV RNA$^+$/p24-Gag$^+$ platelets were measured by FISH–flow cytometry. Bottom left: Boxplot shows percentage of HIV RNA$^+$/p24-Gag$^+$ platelets from healthy donors or HIV-infected individuals on ART detected by FISH–flow cytometry and expressed as a percentage of total platelets in the platelet-rich plasma samples. Normalized percentage values are indicated in italics on the right-hand axis. The quantification threshold (orange dashed line) was established on the basis of healthy donor samples. Samples from HIV-infected individuals on ART were grouped according to the absence (gray, negative) or presence (orange, positive) of HIV in platelets ($P < 0.001$). The number of different individuals tested (n) is shown below the graph. Bottom right: Boxplot shows percentages converted into HIV RNA$^+$/p24-Gag$^+$ platelets per million platelets after data normalization and after subtracting the maximum value obtained from healthy donor control samples. The number of different individuals tested (n) is shown below the graph. Results are from seven independent experiments and are expressed as boxplots generated separately for negative and positive groups. Boxplots represent medians with 25th and 75th percentiles and with minimum/maximum values indicated by whiskers (Mann-Whitney U test). (**C**) Representative confocal microscopy images (top panels) show platelets from HIV-infected individuals on ART immunostained for CD41 (green) and p24-Gag (magenta). Images reconstructed in three dimensions are shown in the bottom panels. White arrowheads indicate HIV contained within platelets. Representative images are shown for platelets from 11 different HIV-infected individuals on ART. Scale bars, 1 μm. (**D**) Representative transmission electron micrograph of an HIV-containing platelet. A viral particle in a small vacuolar compartment is indicated by the magenta box, which is shown at a higher magnification in the image inset. The electron micrograph is representative of samples from five different HIV-infected individuals on ART with viral suppression. (**E**) Immunogold labeling (10 nm) of p24-Gag in cryosections was performed before electron microscopy to confirm the presence of HIV within a platelet compartment (pink arrowhead). Representative image of 10 different images obtained from two different HIV-infected individuals on ART with viral suppression. αG, α-granule; V, vacuole. Scale bars, 0.5 μm, 100 nm, or 50 nm. (**F**) p24-Gag immunofluorescence intensities for platelets from healthy donors or HIV-infected individuals on ART detected by flow cytometry. Results are from seven independent experiments and are expressed as boxplots generated separately for negative and positive groups. Boxplots represent median with 25th and 75th percentiles and with minimum/maximum values indicated by whiskers (Student's t test). (**G**) Image shows green fluorescent protein–positive (GFP$^+$) reporter T cells (green) after interaction with platelet-rich plasma from an HIV-infected individual on ART. Nuclei are labeled with 4',6-diamidino-2-phenylindole (DAPI) (blue); the fluorescence signal (green) was merged with phase contrast (white arrowheads). Scale bar, 10 μm. Boxplot shows the quantification of infectious units per million platelets in platelet-rich plasma samples from HIV-infected individuals on ART who either displayed viremia below LOD or had detectable viral load at the date of sampling. Samples lacking infectious virus are in gray (negative), and those with infectious virus are in orange (positive). The number of different individuals tested (n) is shown below the graph. Results are from eight independent experiments and are expressed as boxplots generated separately for negative and positive groups. Boxplots represent medians with 25th and 75th percentiles and with minimum/maximum values indicated by whiskers (Mann-Whitney U test). ns, not significant.

To identify not only cytosolic HIV RNA but also intact viral particles in platelets, detection of HIV RNA by fluorescence in situ hybridization (FISH) was combined with detection of viral protein p24-Gag by immunofluorescence. Both types of labeling were quantified simultaneously by flow cytometry using a single-cell approach referred to as FISH–flow cytometry (**Fig. 1B** and fig. S2, A to C) (*16*). HIV RNA$^+$/p24-Gag$^+$ FISH–flow cytometry can detect the very low number of latent HIV reservoir cells in HIV-infected individuals on ART, which comprise around 1 infected cell per million CD4$^+$ T cells (*16*–*18*). We found that platelets from HIV-infected individuals on ART that were positive for HIV RNA and p24-Gag comprised 0.1% (CI, 0.047 to 0.15%) of total platelets in the blood of these individuals (**Fig. 1B**, left). When stratified according to either undetectable (below LOD) or detectable viral load at the date of sampling, HIV-infected individuals on ART did not differ in the number of HIV RNA$^+$/p24-Gag$^+$ platelets per 10^6 platelets, which was 1186.99 (CI, 631 to 1600) and 825.8 (CI, 387 to 2676), respectively ($P > 0.05$) (**Fig. 1B**, right). The HIV RNA$^+$/p24-Gag$^+$ signal detected in platelets did not originate from HIV-infected CD4$^+$ T cells (fig. S1D), as T cells obtained from ART-treated HIV-infected individuals did not transcribe HIV RNA in quantities that could be detected by FISH–flow cytometry in the absence of activation by mitogens (*17*).

HIV resides in an internal compartment of platelets

HIV was found inside platelets from HIV-infected individuals on ART as shown by p24-Gag immunolocalization using confocal microscopy (**Fig. 1C** and fig. S3, A and B) and electron microscopy (**Fig. 1, D and E**, and fig. S3, C and D), in parallel with flow cytometry (**Fig. 1F** and fig. S2, A, B, and D). At the confocal microscopy level, HIV appeared to be exclusively confined within closed vacuoles (**Fig. 1C**; p24-Gag detection indicated by arrowheads), as we have previously reported in vitro (*5*, *10*), and did not seem to be associated with the platelet surface. Furthermore, at the ultrastructural level, morphological (**Fig. 1D** and fig. S3C) and immunogold detection of HIV (**Fig. 1E**, p24-Gag detection indicated by arrowhead, and fig. S3D) was restricted to vesicles that were distinct from both the platelet surface and its connected canalicular system, suggesting that HIV was not in contact with the external environment (*8*) or α-granules.

To further validate our microscopy-based immunostaining approaches, p24-Gag$^+$ immunostaining was evaluated by flow cytometry. Differences in p24-Gag$^+$ mean fluorescence intensity were observed for platelets from HIV-infected individuals on ART with (orange bars) or without (gray bars) HIV (**Fig. 1F** and fig. S2, A, B, and D). The HIV p24-Gag protein was detected in platelets from a subset of ART-treated HIV-infected individuals who either were viremic (8 of 25) or had a viral load below the LOD at the date of sampling (17 of 30).

HIV harbored in platelets is replication competent

We next investigated the replication competence of HIV localized in platelets from HIV-infected individuals on ART using a CD4$^+$CCR5$^+$CXCR4$^+$ reporter cell line (*19*, *20*) (**Fig. 1G**). These experiments revealed that in ART-treated HIV-infected individuals with either undetectable (below LOD) or detectable viral load at the date of sampling, a subgroup (**Fig. 1G**, orange) had platelets with similar amounts of infectious viral particles: 2053 infectious units (IU)/10^6 platelets (CI, 1195 to 6013; 11 of 23 individuals) and 1353 IU/10^6 platelets (CI, 533 to 4671; 5 of 14 individuals), respectively (**Fig. 1G**). Among HIV-infected individuals on ART with infectious HIV in platelets and displaying a viral load below LOD at the date of sampling (indicated by crosses in table S3), 72% (8 of 11 tested) were consistently virally suppressed for more than 1 year with a median of 30 (CI, 20 to 50) months before sampling (table S3). This suggested that there was no contamination with residual infectious cell-free virus from blood in the reporter cell assay. Furthermore, in a

individuals on ART with sustained viral suppression were recently shown to contain replication-competent viral DNA (*21*), and megakaryocytes, the precursor cells of platelets, from untreated HIV-infected individuals were shown to harbor HIV RNA (*14*). HIV-1 RNA and HIV virions contained in megakaryocytes could potentially be sequestered by platelets during thrombopoiesis (*11*, *14*, *21*). We detected HIV DNA (fig. S5, A to C) and HIV RNA (fig. S5F) in bone marrow from an HIV-infected individual on ART by in situ hybridization in cells morphologically identified as megakaryocytes. In addition, HIV-integrated proviral DNA was detected in megakaryocytes purified from bone marrow samples from 82% (9 of 11) of HIV-infected individuals on ART with viral suppression (table S4 and fig. S5, D and E), with an estimate of 74.7 (CI, 39 to 140.6) HIV DNA integrated copies per million megakaryocytes (fig. S5, D and E). In platelet-rich plasma samples from the four of these HIV-infected individuals on ART with viral suppression we could analyze, platelets containing HIV RNA and HIV p24-Gag protein were detected (fig. S5G).

To confirm that HIV harbored in platelets was not blood borne, phylogenetic analyses were performed after deep sequencing of HIV *env* V3 sequences in plasma samples from HIV-infected individuals before and after viral suppression. Plasma samples were obtained before viral suppression and were compared to peripheral blood mononuclear cells (PBMCs) and platelet samples after up to 69 months of viral suppression by ART. These phylogenetic analyses demonstrated that after viral suppression, platelet-associated HIV originated from a different compartment than did PBMC-associated HIV provirus or HIV in plasma before ART suppression (fig. S6A). In addition, translated sequences revealed a shift in HIV tropism from CCR5 variants in plasma before ART treatment to CXCR4 variants in PBMCs and platelets after viral suppression by ART. The independent grouping of platelet-derived CXCR4 variants (fig. S6, A and B) in the phylogenetic analysis demonstrated that HIV in platelets did not originate from a latent reservoir established before ART or from the $CD4^+$ T cell latent reservoir (*22*, *23*). More longitudinal, in-depth phylogenetic studies on HIV genome sequences obtained from platelets, bone marrow, and $CD4^+$ T cells of HIV-infected individuals before and after viral suppression will be required to confirm this finding.

HIV harbored in platelets can be transferred to macrophages in vitro

At the end of their short life span, platelets are ultimately phagocytosed by mononuclear phagocytic cells residing mainly in the liver and spleen (*24*). Tissue macrophages are central to this process by engulfing senescent and apoptotic platelets via integrins including $\alpha_{IIb}/\beta3$ and scavenger receptors (*24*–*27*). HIV harbored in platelets could be transferred to tissue macrophages through this process of platelet elimination. Therefore, we next investigated whether HIV-containing platelets could be phagocytosed by macrophages in vitro (**Fig. 2**, fig. S7, and movie S1). HIV-containing platelets from HIV-infected individuals on ART with viral load consistently below LOD for 52.5 (CI, 12 to 75) months were found to adhere to and, in turn, be phagocytosed by macrophages in vitro (**Fig. 2, A and B**, and movie S1). This resulted in integration of HIV proviral DNA into the genome of macrophages with 48.25 (CI, 5.24 to 183.9) proviral HIV DNA copies per million macrophages (**Fig. 2C**). Infection appeared to be productive as these HIV-infected macrophages, in turn, produced infectious HIV virions (**Fig. 2D**). HIV proviral DNA integration and infectious virus production in vitro could be inhibited by preventing platelet-macrophage interactions using abciximab, a platelet-specific anti–integrin $\alpha_{IIb}/\beta3$ Fab (**Fig. 2, C and D**, and fig. S7, B to D).

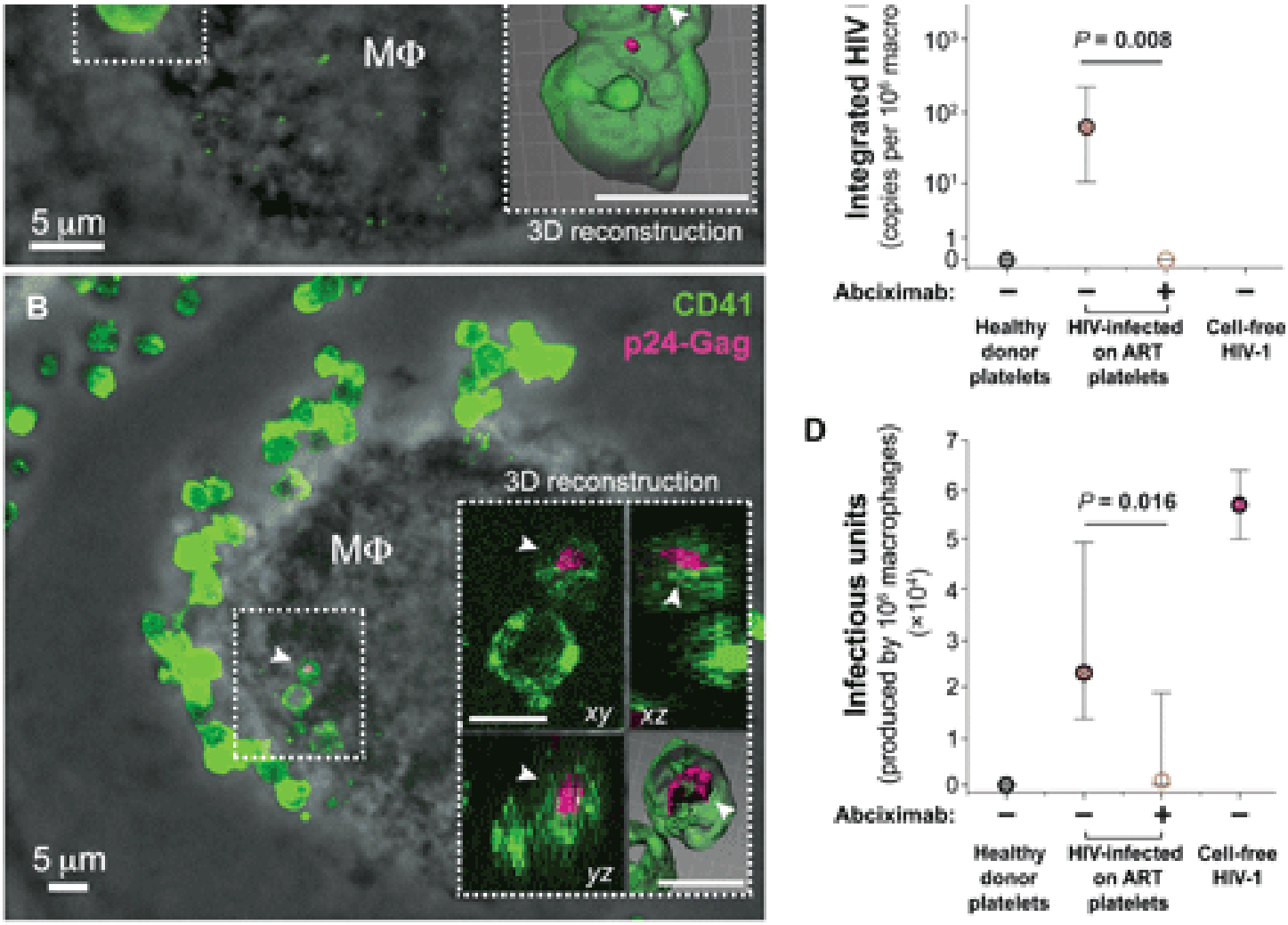

Download high-res image | Open in new tab | Download Powerpoint

Fig. 2 Transfer of HIV from platelets to macrophages in vitro.

(**A** and **B**) Representative confocal microscopy images of HIV-containing platelets interacting with macrophages (MΦ) in vitro after immunostaining for CD41 (green) and p24-Gag (pink); image is merged with phase-contrast image. White arrowheads show labeled virus within platelets. Image insets show three-dimensional reconstructions or projections in *xy*, *yz*, and *xz* dimensions for HIV-containing platelets. Images are representative of five different individuals. Scale bars, 5 μm (main and inset figures). (**C**) Number of integrated copies of HIV DNA per 10^6 macrophages after 7 days of coculture with platelets from HIV-infected individuals on ART with viral suppression in the presence (solid orange circle) or absence (empty orange circle) of abciximab. Culture with cell-free HIV-1 was used as a positive control (magenta circle), and healthy donor platelets were used as a negative control (gray circle). (**D**) Infectious units produced per 10^6 macrophages after 7 days of coculture with platelets from HIV-infected individuals on ART with viral suppression in the presence (solid orange circle) or absence (empty orange circle) of abciximab. Culture with cell-free HIV-1 was used as a positive control (magenta circle), and healthy donor platelets were used as a negative control (gray circle). Results for (C) and (D) are presented as medians (circles) with 95% CIs (whiskers). Data represent three independent experiments with samples from five different HIV-infected individuals on ART. Mann-Whitney *U* test was applied for paired experimental data for platelets from HIV-infected individuals on ART, treated or not treated with abciximab in vitro.

HIV-infected individuals on ART with platelets containing HIV have low CD4$^+$ T cell counts

Next, we compared clinical characteristics at the date of sampling between HIV-infected individuals on ART who did (orange bars) or who did not (gray bars) have HIV-containing platelets (table S2 and Fig. 3A). HIV-infected individuals on ART with HIV-containing platelets had a low CD4$^+$ T cell count (<350/μl) that was threefold less compared to HIV-infected individuals on ART without HIV-containing platelets (Fig. 3A). In contrast, the presence of HIV-containing platelets was not associated with total lymphocyte counts or platelet counts, age, years since diagnosis, years on ART (fig. S8, A to C), or the type of ART regimen (table S5). We performed a multivariate analysis of the clinical characteristics of HIV-infected individuals with or without HIV in platelets at the date of sampling. Principal component analysis (PCA) showed separate clusters for blood samples with or without HIV-containing platelets (Fig. 3B). This distribution was mainly driven by principal component (dimension) 2, where CD4$^+$ T cell count was the strongest contributor (fig.

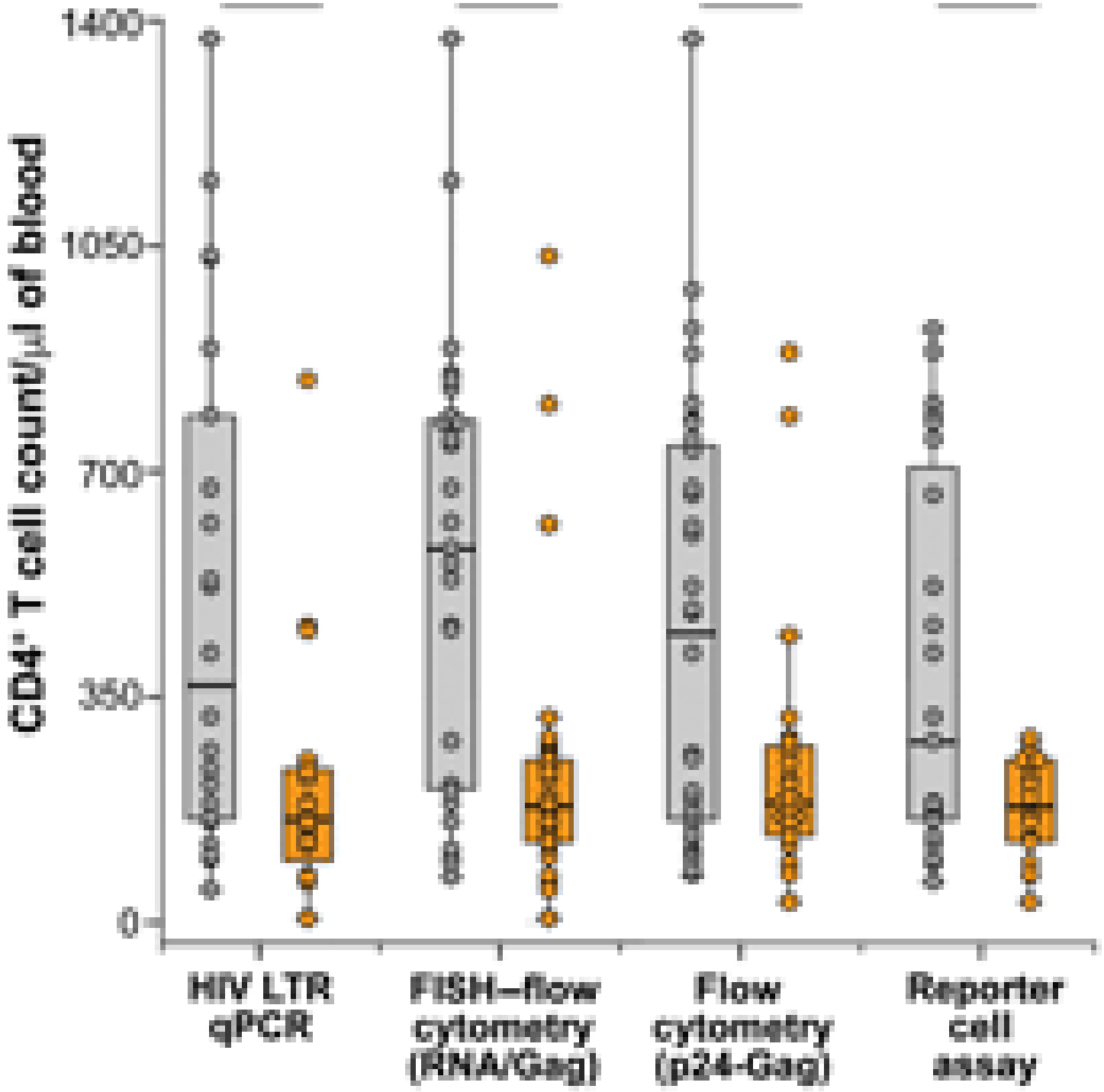

B

Negative Positive

Variable vectors

3

CD4+ T cell count

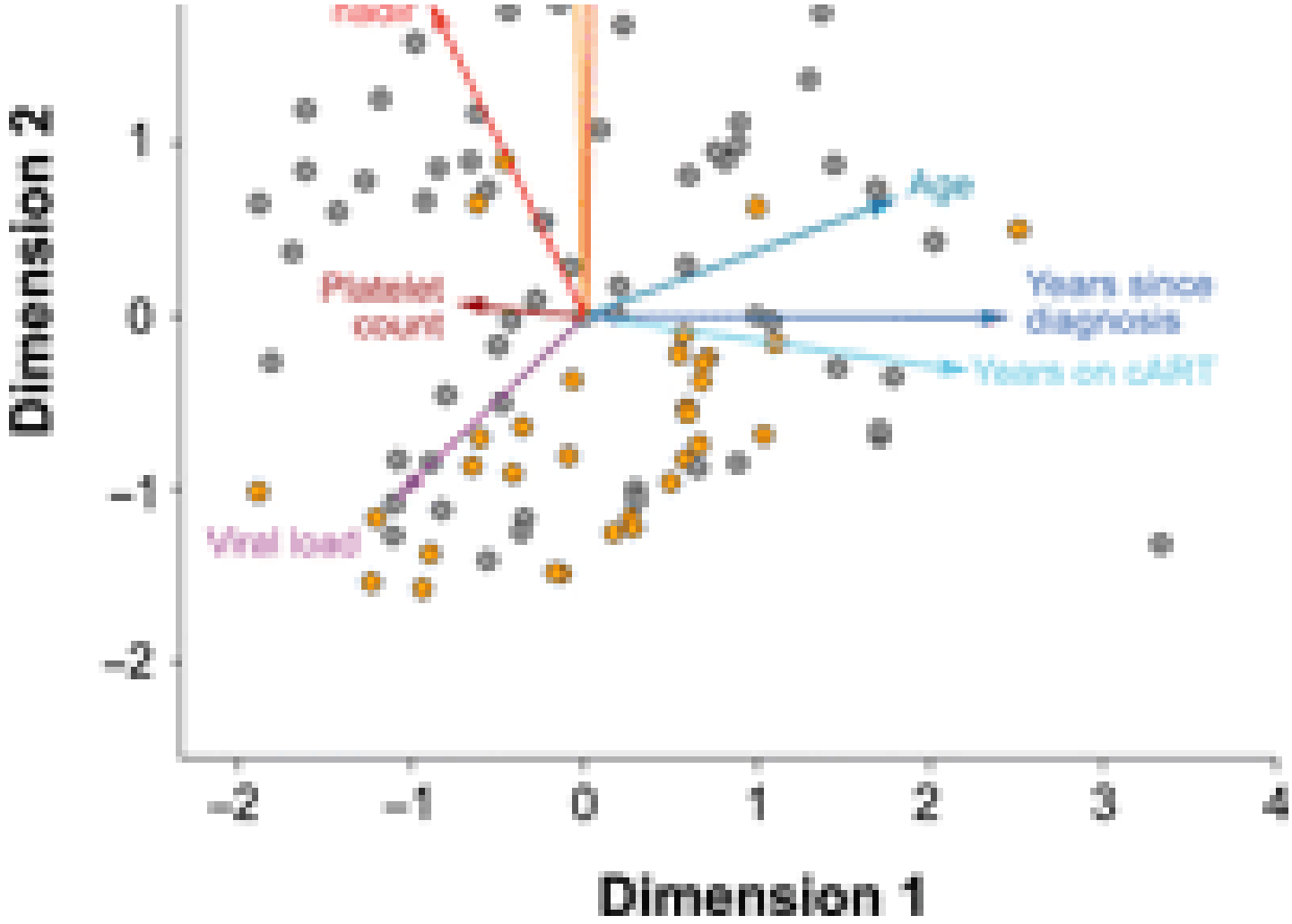

Download high-res image | Open in new tab | Download Powerpoint

Fig. 3 Platelets containing HIV correlate with low CD4⁺ T cell counts.

(**A**) Comparison of CD4⁺ T cell counts at the date of sampling for HIV-infected individuals on ART whose platelets either contained (positive, orange) or did not contain (negative, gray) HIV. HIV was detected by HIV LTR qPCR, FISH flow cytometry (HIV RNA⁺/p24-Gag⁺), p24-Gag flow cytometry, and a reporter T cell assay in seven, five, seven, and eight independent experiments, respectively. HIV-infected individuals on ART with HIV-containing platelets (orange) showed lower CD4⁺ T cell counts (<350/μl) than did those with platelets lacking HIV (gray). Results are shown as boxplots generated separately for positive and negative groups. The Mann-Whitney *U* test was used to compare negative (gray) and positive (orange) groups for each HIV detection technique. (**B**) PCA of samples from HIV-infected individuals on ART categorized according to the presence (positive, orange) or absence (negative, gray) of HIV in platelets. These data and the clinical characteristics for each HIV-infected individual at the date of sampling are represented as variable vectors (arrows).

HIV-infected individuals on ART with platelets containing HIV show immunological failure

To address the potential clinical implications of platelets containing HIV, a subset of 35 HIV-infected individuals on ART analyzed above was selected (**Table 1**). Selection was based on two criteria, namely, HIV detection in platelets using at least two different techniques (tables S2) and unambiguous clinical data available for 1 year before the date of sampling. In these selected HIV-infected individuals on ART, the historical CD4⁺ T cell nadir, a clinical characteristic critical for immune recovery (*28*), was significantly lower (<200 cells/μl) in those with HIV-containing platelets compared to those without HIV-containing platelets ($P = 0.006$, **Fig. 4A**). A sustained low CD4⁺ T cell count (<350 cells/μl), irrespective of viral suppression, persisted in HIV-infected individuals on ART with HIV-containing platelets. In contrast, HIV-infected individuals on ART lacking HIV in platelets had a CD4⁺ T cell count above this threshold, especially if they were aviremic. This was shown by analysis of mean CD4⁺ T cell counts at the date of sampling and during a retrospective and prospective 18-month period before and after sampling (**Fig. 4B**). These results indicated that the presence of HIV harbored in platelets correlated with immunological failure, which was defined as HIV-infected individuals on ART whose CD4⁺ T cell counts remained <350 cells/μl for more than one year (*29*).

least 1 year before sampling. Uncontrolled viremia was defined as >1.60 HIV RNA $\log_{10}$ copies/ml of plasma at the date of sampling or less than 12 months of continuous viral suppression.

View this table: **View popup** | **View inline**

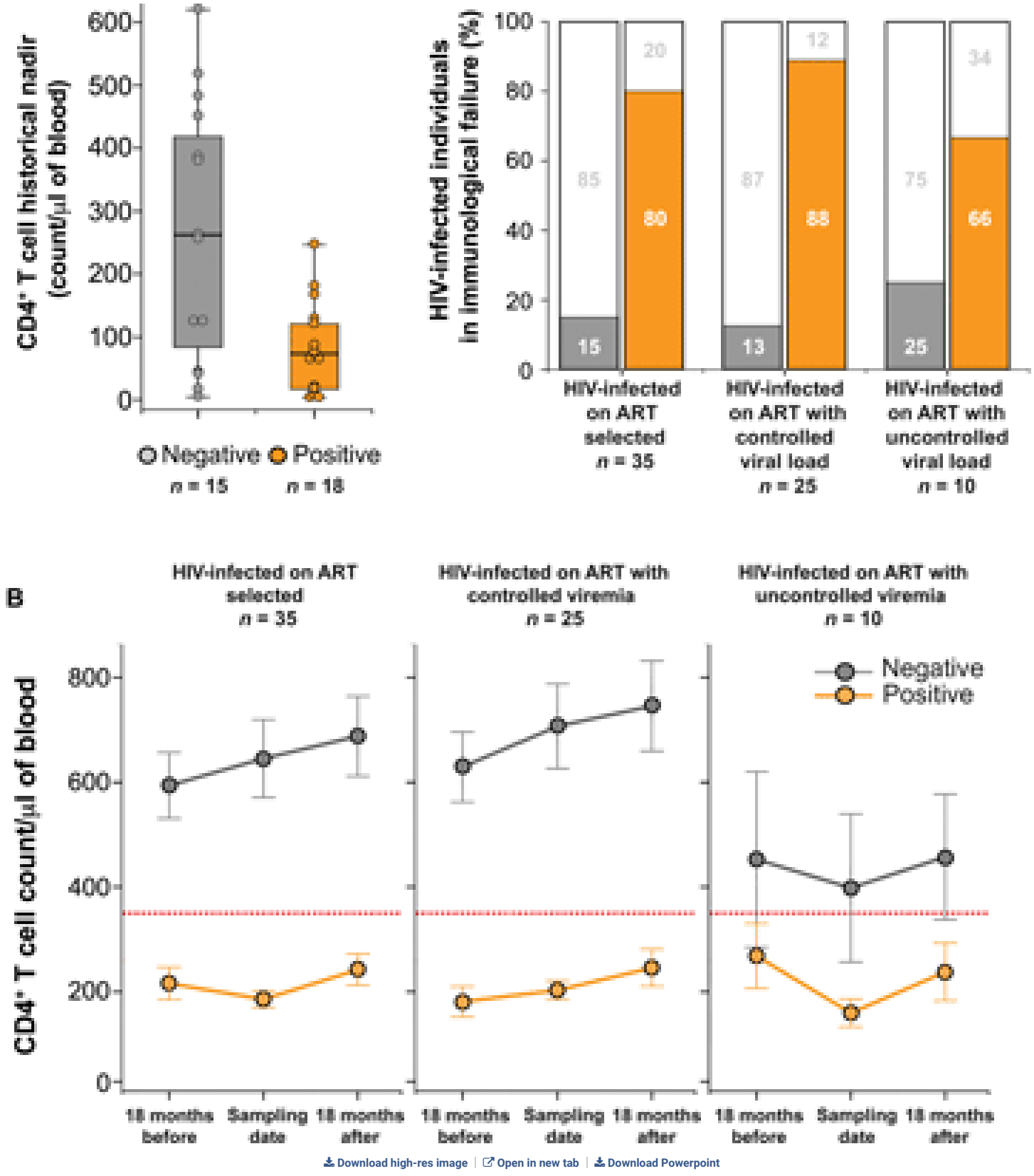

Fig. 4 Platelets containing HIV correlate with poor immunological recovery.

(**A**) $CD4^+$ T cell counts (historical nadir) for HIV-infected individuals on ART whose platelets either did (orange, positive) or did not (gray, negative) contain HIV. HIV-infected individuals on ART with HIV-containing platelets had a lower mean $CD4^+$ T cell count nadir (<200 cells/μl) compared to the negative group ($P = 0.006$, Mann-Whitney U test). The number of individuals (n) is shown below the graph. (**B**) Mean $CD4^+$ T cell counts for HIV-infected individuals on ART who were positive (orange line) or negative (gray line)

We found that 80% of the HIV-infected individuals on ART with HIV-containing platelets (**Fig. 4C**, orange bars) were in immunological failure compared to only 15% of HIV-infected individuals on ART without HIV-containing platelets (**Fig. 4C**, gray bars). HIV-infected individuals on ART with HIV-containing platelets had a >20-fold higher chance of failing to recover $CD4^+$ T cell counts to above 350 cells/μl, compared to those without HIV in their platelets (odds ratio, 22.6; CI, 3.8 to 132.1; $P = 0.0005$). The likelihood of immunological failure for HIV-infected individuals on ART with viral suppression and HIV-containing platelets was higher (odds ratio, 56; CI, 4.3 to 719.2; $P = 0.002$) compared to those who were viremic at the date of sampling or displayed less than 12 months of continuous viral suppression (odds ratio, 6; CI, 0.3 to 101.5; $P = 0.21$) (**Table 1** and table S6).

DISCUSSION

We have shown here that platelets from HIV-infected individuals on ART with sustained low $CD4^+$ T cell counts harbor replication-competent HIV and do so despite viral suppression below LOD. Our results show that in platelets, HIV is confined to an intracellular compartment analogous to the virus-containing compartments typically formed in HIV-infected myeloid cells in vitro (*30*) and in vivo (*31*, *32*). These compartments are functionally distinct from the cell endosomal system, providing a shelter for the virus against the direct action of neutralizing antibodies, cytoplasmic innate immunity sensors, and the late endosomal/lysosomal degradative environment (*30*). Accordingly, platelets harboring HIV in these privileged compartments could preserve virus integrity throughout their 8- to 10-day life span.

The HIV in platelets that we report could have originated from direct endocytosis of HIV in the circulation of viremic patients by platelets (*7*, *10*). However, the presence of intact, replication-competent virus in platelets from individuals on ART with viral loads below LOD for long periods suggests that platelets may associate with HIV in an active viral replication niche. HIV-infected megakaryocytes that we found in HIV-infected individuals on ART with low $CD4^+$ T cell counts potentially could be the source of HIV-containing platelets.

Platelets are short-lived, anuclear blood components lacking the nuclear machinery to meet the recent criteria used to define HIV latent reservoirs (*23*). These criteria include display of integrated proviral DNA and rebound of virus production upon interruption of ART. Instead, platelets and perhaps other blood cells (*33*, *34*) may participate in HIV transmission and persistence by sheltering the virus from the immune response. The T cell latent reservoir is long-lived and harbors integrated HIV DNA. We suggest that platelets harboring HIV can carry HIV RNA and transport replication-competent virus. Platelets would thus form a transient shelter for HIV in the blood of some HIV-infected individuals on ART and could promote infection by delivering virus to target cells such as macrophages as we have shown here in vitro. Furthermore, our study suggests that HIV may associate with platelets during thrombopoiesis in the HIV-infected bone marrow megakaryocytes of HIV-infected individuals virally suppressed by ART with low $CD4^+$ T cell counts.

A potential platelet-mediated pathway for viral dissemination during ART may correlate with sustained immunological failure, although the causative nature of this correlation remains to be established. The poor immunological recovery observed in ART-treated HIV-infected individuals may be driven by persistent inflammation associated with T cell immune dysfunction (*35*–*37*). Residual inflammation markers in blood, such as d-dimers and interleukin-6 (IL-6) detected in plasma, do not correlate with immunological failure (*38*) and thus are unlikely to have an impact on the association of HIV with platelets. Inflammation-driven T cell dysfunction could result from the low residual production of HIV by latent reservoirs such as tissue macrophages (*31*, *39*). Further studies are necessary to elucidate the molecular and cellular mechanisms connecting immunological failure to platelets containing HIV.

Twenty percent to 30% of HIV-infected individuals are unable to reconstitute a competent immune system despite adherence to ART and a viral load below LOD (*29*, *35*, *40*, *41*); no therapeutic strategy is available to improve their immune recovery (*41*, *42*). Systematic clinical studies will be required to demonstrate the potential predictive value of detecting HIV-containing platelets in individuals in immunological failure for the purpose of anticipating appropriate therapeutic interventions. Our results suggest that abciximab, an antiplatelet agent already in clinical use, could block viral dissemination to macrophages by HIV-containing platelets.

Our study has a number of limitations. Further studies are needed to elucidate how HIV shelters in the platelets of HIV-infected individuals on ART despite viral suppression and the association of HIV-containing platelets with $CD4^+$ T cell recovery failure. Although our study analyzed samples from 80 HIV-infected individuals on ART, limited sample amounts did not allow testing of every sample with all four techniques we used for detecting HIV in platelets. Samples from a greater number of HIV-infected individuals on ART and longitudinal samples from the same individuals at 1-year intervals should be studied to confirm our results and to establish functional correlations between the presence of HIV in platelets and immunological failure. The finding of HIV virions identified at the ultrastructural level in some platelets needs to be confirmed by directly correlating p24-Gag immunolabeling detected by confocal microscopy with that identified by electron microscopy. Additional immunolabeling experiments will need to be performed to identify the compartment in platelets in which HIV resides and if it is similar to the HIV compartment in HIV-infected macrophages (*31*). The activation status of platelets interacting with macrophages during HIV transfer remains to be determined as well as whether a specific tissue macrophage subset is selectively targeted. To prove our hypothesis that HIV-infected platelets are derived from HIV-infected megakaryocytes, comparative sequencing of HIV *env* V3 will need to be performed on blood T cells, megakaryocytes, and platelets both before ART and after 1 year on ART with consistent blood viral suppression.

Study design

Our study investigated whether replication-competent HIV resided within platelets from HIV-infected individuals on ART. The HIV-infected individuals on ART who participated in this study belonged to a large prospective cohort of HIV-infected individuals of at least 15 years of age from the French Hospital Database on HIV created in 1989. These HIV-infected individuals received care at the Ambroise Paré and Raymond Poincaré Hospitals that are among 70 participating centers in the French Hospital Database on HIV. The only enrollment criterion for the French Hospital Database on HIV was documented HIV-1 or HIV-2 infection. Written informed consent was obtained for all study participants, and data submitted by the participating centers were anonymized and encrypted. The French Hospital Database on HIV was approved by the French national institutional ethics committee (Commission Nationale de l'Informatique et des Libertés) on 27 November 1991. Human samples in this study were used in accordance with the World Medical Association Declaration of Helsinki. Ethical authorization for obtaining postmortem bone marrow samples through whole-body donation from uninfected and ART-treated HIV-infected individuals was provided by the State University of New Jersey and The University of Texas Medical Branch, with Institutional Review Board (IRB) authorization numbers of Pro20140000794/Pro2012001303 and 18-0136/18-0134, respectively.

Platelet-rich plasma samples used in this study were obtained during routine blood testing of 80 HIV-infected individuals on ART from the French Hospital Database on HIV, who received care at the Ambroise Paré and Raymond Poincaré Hospitals. The enrollment criterion for these HIV-infected individuals was that ART had been initiated for at least 1 year before the time of blood sampling. Viremia was regularly tested in human plasma samples using the Abbott RealTime HIV-1 assay on an automated m2000 system. This allowed detection of HIV RNA copies per milliliter of plasma with a range of 1.6 $\log_{10}$ copies (40 copies) to 7 $\log_{10}$ copies. Values below the LOD of 1.6 $\log_{10}$ copies/ml were considered to reflect undetectable viremia. Tables S1 and S2 present the following clinical information for study participants: viral load ($\log_{10}$ HIV copies per milliliter of blood), total lymphocyte counts (10^6/ml of blood), $CD4^+$ T cell counts and historical nadir (cells per microliter of blood), and platelet counts (10^6/ml of blood). Table S5 shows the ART regimens for study participants.

It should be noted that the HIV-infected individuals on ART in our study were seen in a hospital setting and may not be representative of the HIV-infected population seen in local clinics. Therefore, the immunological nonresponders in the HIV-infected cohort we analyzed may not be representative of immunological failure in the broader HIV-infected population on ART.

Human peripheral blood and platelet-rich plasma samples from healthy HIV-seronegative donors were obtained from the French blood collection center (Paris, France). Platelet-rich plasma from healthy donors was used as a negative control for all experiments and was processed using the same methods as for platelet-rich plasma from HIV-infected individuals.

Platelet-rich plasma collection

Peripheral blood samples were obtained from donors by venipuncture into plastic tubes containing anticoagulant EDTA. Samples were centrifuged for 10 min at 160*g* and 22°C for blood fractionation, allowing for clear separation of platelet-rich plasma from whole blood. To avoid potential contamination by rare leukocytes, the upper two-thirds of the platelet-rich plasma fraction were carefully collected and transferred to new plastic tubes as recommended for functional analyses (***43***). Platelet-poor plasma was obtained after centrifugation of platelet-rich plasma at 1100*g*, 10 min, room temperature, and collection of supernatants.

Platelet-rich plasma fractions were frozen at −80°C until used in the experiments (***44***). We verified by flow cytometry that (i) viable $CD41^+$ platelets represent >70% of total events recorded in platelet-rich plasma, (ii) >90% of $CD41^+$ platelets conserved $CD42b^+$ membrane staining after thawing, and (iii) thawing does not increase the number of activated platelets characterized by $CD62P^+$ immunostaining, with platelet-rich plasma samples displaying 49.2 and 51% of activated platelets ($CD41^+CD62P^+$) before and after thawing, respectively.

Quantitative PCR

qPCR of HIV-1 long terminal repeat (LTR) RNA sequences was performed from platelet pellets obtained after centrifugation of 500 µl of platelet-rich plasma at 1100*g*, 10 min, at room temperature. Platelet RNA was obtained as described (***45***) and processed for qPCR TaqMan assay using LTR-specific primer (Vi03453409_s1, Thermo Fisher Scientific Inc.) labeled with a FAM-MGB probe on an Applied Biosystems TaqMan RNA-to-Ct 1-Step Kit protocol (Thermo Fisher Scientific Inc.). RNA from platelet-rich plasma samples was eluted into 15 µl of nuclease-free water, and 5 µl of this eluate was used per qPCR reaction. Platelet-rich plasma RNA samples display an average A260/280 ratio of 1.82 (CI, 1.65 to 2.01), indicating good RNA quality (high quality = ~2 A260/280 ratio according to technique standards). The mean amount of RNA applied per reaction was 63.39 ng (CI, 42.5 to 85.2), which fits into the range of specific detection of the qPCR reagents. Reaction and data acquisition were performed using a LightCycler 480 II (Roche). The number of HIV LTR copies per million platelets was calculated on the basis of platelet-rich plasma platelet counts and qPCR crossing point (Cp) values obtained from a standard curve using a full-length molecular clone of HIV-1 pNL4-3 strain.

Contamination of platelet-rich plasma samples with lymphocytes was assessed by detection of the lymphocyte-specific CD3δ transcript (***46***) in platelet-rich plasma by qPCR TaqMan assay using CD3δ primer (Hs00174158_m1, Thermo Fisher Scientific Inc.) labeled with FAM-MGB probe on an Applied Biosystems TaqMan RNA-to-Ct 1-Step Kit protocol (Thermo Fisher Scientific Inc.). The number of lymphocytes was calculated on the basis of Cp values obtained from a standard curve using serial dilutions of RNA obtained from known amounts of $CD4^+$ T cells.

anti-p24 antibody (1:20, KC57 clone, Beckman Coulter Inc.) coupled to fluorescein isothiocyanate (FITC) and anti-CD41/CD61 antibody coupled to phycoerythrin (PE) (1:20, A2A9/6 clone, BioLegend Inc.).

Flow cytometry analyses of platelets processed for FISH (FISH–flow cytometry) were performed under the Guava easyCyte high-throughput system version 6HT2L (Merck Millipore, Merck, KGaA) set to very low flow rate (0.12 µl/s) and laser gains of 3.5 (GRN-B laser line), 4.3 (YEL-B laser line), and 7.6 (RED-R laser line) in a range of 1 to 1024 units.

The gating strategy to retrieve HIV RNA$^+$/p24-Gag$^+$ double-positive platelets (fig. S2, A to C) was established in InCyte (Merck Millipore, Merck, KGaA) software consisting in (i) gating the population of single platelets based on forward and side scatter (in log/log scale, forward scatter (FSC) threshold value = 100), (ii) then gating on CD41$^+$ events after applying a threshold based on isotype controls, and (iii) calculating CD41$^+$ events according to p24 immunostaining and HIV RNA probe hybridization as described (*16*, *47*). Data normalization was performed by subtracting the maximum percentage acquired in n = 12 healthy donor samples from the percentages acquired in patient samples per experiment.

FISH–flow cytometry method was also applied as described (*17*) for detection of HIV RNA$^+$/p24-Gag$^+$ PBMCs, isolated from blood buffy coats of cART-treated or chronically infected nontreated HIV-infected patients after Ficoll-Hypaque density gradient centrifugation.

Retrospective and prospective analysis of clinical parameters

We categorized ART-treated HIV-infected individuals in two groups according to the presence (positive) or absence (negative) of HIV in platelets. Classification of these individuals as positive or negative was based on similar results obtained in at least two different techniques used for detection of HIV-containing platelets. CD4$^+$ T cell historical nadir, age, years since HIV diagnosis, and years since treatment of patients from the positive and negative groups were compared using statistical methods as described below. From this group of patients classified as positive or negative for HIV in platelets, we selected those 35 individuals for which we could collect longitudinal CD4$^+$ T cell count and viral load measurements (**Table 1**). Clinical parameters of these 35 individuals with consistent detection of HIV in platelets were used for retrospective and prospective analyses presented in **Fig. 4**.

The retrospective and prospective analyses of patient clinical information refer to a period of several months around the date of sampling. When indicated, patients were categorized in controlled viral load group (patients presenting HIV RNA copies per milliliter of plasma always below LOD for at least 1 year before sampling) or noncontrolled viral load group (patients presenting >1.60 $\log_{10}$ copies of HIV RNA per milliliter of plasma at date of sampling or displaying less than 12 months of continuous suppression). Regarding immunological status, patients were categorized as immunologically competent when CD4$^+$ T cell count was >350 cells/µl for two or more consecutive measurements, or in immunological failure when CD4$^+$ T cells per microliter was constantly <350 cells/µl for all blood sample collected for at least 1 year including the date of sampling for HIV in platelets. We obtained, for each selected patient, a mean CD4$^+$ T cell number for counts registered 18 months before sampling (retrospective count) and for 18 months after sampling (prospective count). **Figure 4B** shows the mean retrospective CD4$^+$ T cell count, the mean CD4$^+$ T cell count at sampling date, and the mean prospective CD4$^+$ T cell count of patients in which CD4$^+$ T cell count was surveyed.

Statistical analysis

In all HIV detection assays performed, blood and platelet-rich plasma samples were stratified into two groups (positive or negative) according to the presence or absence of HIV in platelets. Median numbers of HIV-containing platelets per milliliter of blood were calculated exclusively from samples of the positive group. Results are expressed as median, followed by the 95% CI. Boxplots represent median (central line in the box) with 25th and 75th percentiles (box edges) and with minimum/maximum values (upper and lower whiskers).

All statistical analyses were performed using IBM SPSS Statistics software (IBM). Pairwise comparisons of normal distributions were performed using a Student's t test. Pairwise and multiple comparisons of non-normal distributions were performed using the nonparametric tests Mann-Whitney U and Kruskal-Wallis, respectively. Clinical characteristics of HIV-infected individuals at the date of sampling were examined by multivariate analysis using PCA, a data reduction technique that simultaneously quantifies categorical variables while reducing the dimensionality of the data. Results are presented as a two-dimensional PCA plot (biplot), a graphical display that illustrates the relationships among the components, original variables, and observations (*48*). Clinical information obtained at the date of sampling was normalized to remove bias from the analysis. In the biplot, clinical characteristics are shown as variable vectors (component loading). Samples (objects in the biplot) were labeled according to experimental detection (positive) or lack of detection (negative) of HIV in platelets.

Repetition of parameter values from clinical histories due to multiple samplings (e.g., CD4$^+$ T cell nadir) did not interfere with the PCA performed, because random selection of one sample per HIV-infected individual before running the PCA did not change the results. Multinomial logistic regression was performed using detection of HIV in platelets as a dependent variable and clinical parameters at the date of sampling as covariates but excluding CD4$^+$ T cell historical nadir due to colinearity with CD4$^+$ T cell counts (Pearson's coefficient = 0.635, $P < 0.001$). Fisher's exact test was used for odds ratio and risk estimates. $P < 0.05$ was considered significant.

SUPPLEMENTARY MATERIALS

stm.sciencemag.org/cgi/content/full/12/535/eaat6263/DC1

Fig. S3. HIV-containing platelets detected by electron and confocal microscopy.

Fig. S4. Infection of macrophages by HIV in platelets is due to direct interactions and not residual cell-free viruses present in platelet-rich plasma.

Fig. S5. HIV-1 integrated proviral DNA in megakaryocytes from HIV-infected individuals on ART with viral suppression.

Fig. S6. Deep sequencing and phylogenetic analysis of HIV *env* V3 segments before and after viral suppression in the same HIV-infected individuals on ART.

Fig. S7. Interaction between platelets and macrophages is blocked by the anti–integrin αII/β3 Fab abciximab.

Fig. S8. Detection of HIV-containing platelets does not correlate with other clinical characteristics.

Table S1. Clinical information on HIV-infected individuals on ART analyzed for HIV in platelets.

Table S2. Clinical information on each HIV-infected individual on ART analyzed for HIV in platelets.

Table S3. Available viral load measurements for HIV-infected individuals on ART positive for HIV in platelets and with a viral load below the LOD at the date of sampling.

Table S4. Clinical information for each HIV-infected individual on ART analyzed for HIV in megakaryocytes.

Table S5. ART regimens for HIV-infected individuals classified as positive or negative for the presence of HIV in platelets.

Table S6. $CD4^+$ T cell counts and viral load measurements for HIV-infected individuals on ART with controlled viremia and positive for HIV in platelets.

Table S7. List of Gag mRNA probe sequences used for FISH–flow cytometry.

Data file S1. Individual-level data for **Figs. 1**, **2**, and **4** and figs. S1, S4, and S7.

Movie S1. Laser scanning confocal microscopy image of an HIV-containing platelet being engulfed by a macrophage.

References (*49*–*68*)

Appendix

View/request a protocol for this paper from *Bio-protocol*.

REFERENCES AND NOTES

1. J. W. Semple, J. E. Italiano Jr.., J. Freedman, Platelets and the immune continuum. *Nat. Rev. Immunol.* **11**, 264–274 (2011). CrossRef PubMed Google Scholar
2. O. Garraud, F. Cognasse, Are platelets cells? And if yes, are they immune cells? *Front. Immunol.* **6**, 70 (2015). CrossRef PubMed Google Scholar
3. A. Assinger, Platelets and infection - an emerging role of platelets in viral infection. *Front. Immunol.* **5**, 649 (2014). CrossRef PubMed Google Scholar
4. J. R. Ariede, M. I. Pardini, G. F. Silva, R. M. Grotto, Platelets can be a biological compartment for the hepatitis C virus. *Braz. J. Microbiol.* **46**, 627–629 (2015). Google Scholar
5. S. Boukour, J. M. Massé, L. Bénit, A. Dubart-Kupperschmitt, E. M. Cramer, Lentivirus degradation and DC-SIGN expression by human platelets and megakaryocytes. *J. Thromb. Haemost.* **4**, 426–435 (2006). CrossRef PubMed Google Scholar
6. A. Chabert, H. Hamzeh-Cognasse, B. Pozzetto, F. Cognasse, M. Schattner, R. M. Gomez, O. Garraud, Human platelets and their capacity of binding viruses: Meaning and challenges? *BMC Immunol.* **16**, 26 (2015). CrossRef PubMed Google Scholar
7. C. Chaipan, E. J. Soilleux, P. Simpson, H. Hofmann, T. Gramberg, A. Marzi, M. Geier, E. A. Stewart, J. Eisemann, A. Steinkasserer, K. Suzuki-Inoue, G. L. Fuller, A. C. Pearce, S. P. Watson, J. A. Hoxie, F. Baribaud, S. Pöhlmann, DC-SIGN and CLEC-2 mediate human immunodeficiency virus type 1 capture by platelets. *J. Virol.* **80**, 8951–8960 (2006). Abstract/FREE Full Text Google Scholar
8. C. Flaujac, S. Boukour, E. Cramer-Bordé, Platelets and viruses: An ambivalent relationship. *Cell. Mol. Life Sci.* **67**, 545–556 (2010). CrossRef PubMed Google Scholar
9. A. Y. Simon, M. R. Sutherland, E. L. Pryzdial, Dengue virus binding and replication by platelets. *Blood* **126**, 378–385 (2015). Abstract/FREE Full Text Google Scholar

12. T. H. Lee, R. R. Stromberg, J. W. Heitman, L. Sawyer, C. V. Hanson, M. P. Busch, Distribution of HIV type 1 (HIV-1) in blood components: Detection and significance of high levels of HIV-1 associated with platelets. *Transfusion* **38**, 580–588 (1998). Google Scholar

13. T. H. Lee, R. R. Stromberg, D. Henrard, M. P. Busch, Effect of platelet-associated virus on assays of HIV-1 in plasma. *Science* **262**, 1585–1586 (1993). FREE Full Text Google Scholar

14. D. Zucker-Franklin, Y. Z. Cao, Megakaryocytes of human immunodeficiency virus-infected individuals express viral RNA. *Proc. Natl. Acad. Sci. U.S.A.* **86**, 5595–5599 (1989). Abstract/FREE Full Text Google Scholar

15. S. G. Deeks, S. R. Lewin, A. L. Ross, J. Ananworanich, M. Benkirane, P. Cannon, N. Chomont, D. Douek, J. D. Lifson, Y.-R. Lo, D. Kuritzkes, D. Margolis, J. Mellors, D. Persaud, J. D. Tucker, F. Barre-Sinoussi; International AIDS Society Towards a Cure Working Group, G. Alter, J. Auerbach, B. Autran, D. H. Barouch, G. Behrens, M. Cavazzana, Z. Chen, É. A. Cohen, G. M. Corbelli, S. Eholié, N. Eyal, S. Fidler, L. Garcia, C. Grossman, G. Henderson, T. J. Henrich, R. Jefferys, H.-P. Kiem, J. M. Cune, K. Moodley, P. A. Newman, M. Nijhuis, M. S. Nsubuga, M. Ott, S. Palmer, D. Richman, A. Saez-Cirion, M. Sharp, J. Siliciano, G. Silvestri, J. Singh, B. Spire, J. Taylor, M. Tolstrup, S. Valente, J. van Lunzen, R. Walensky, I. Wilson, J. Zack, International AIDS society global scientific strategy: Towards an HIV cure 2016. *Nat. Med.* **22**, 839–850 (2016). CrossRef Google Scholar

16. A. E. Baxter, J. Niessl, R. Fromentin, J. Richard, F. Porichis, M. Massanella, N. Brassard, N. Alsahafi, J. P. Routy, A. Finzi, N. Chomont, D. E. Kaufmann, Multiparametric characterization of rare HIV-infected cells using an RNA-flow FISH technique. *Nat. Protoc.* **12**, 2029–2049 (2017). CrossRef Google Scholar

17. A. E. Baxter, J. Niessl, R. Fromentin, J. Richard, F. Porichis, R. Charlebois, M. Massanella, N. Brassard, N. Alsahafi, G. G. Delgado, J. P. Routy, B. D. Walker, A. Finzi, N. Chomont, D. E. Kaufmann, Single-cell characterization of viral translation-competent reservoirs in HIV-infected individuals. *Cell Host Microbe* **20**, 368–380 (2016). CrossRef PubMed Google Scholar

18. J. Grau-Exposito, C. Serra-Peinado, L. Miguel, J. Navarro, A. Curran, J. Burgos, I. Ocaña, E. Ribera, A. Torrella, B. Planas, R. Badía, J. Castellví, V. Falcó, M. Crespo, M. J. Buzon, A novel single-cell fish-flow assay identifies effector memory CD4+ T cells as a major niche for HIV-1 transcription in HIV-infected patients. *MBio* **8**, e00876-17 (2017). Abstract/FREE Full Text Google Scholar

19. C. Hess, T. Klimkait, L. Schlapbach, V. Del Zenero, S. Sadallah, E. Horakova, G. Balestra, V. Werder, C. Schaefer, M. Battegay, J. A. Schifferli, Association of a pool of HIV-1 with erythrocytes in vivo: A cohort study. *Lancet* **359**, 2230–2234 (2002). CrossRef PubMed Web of Science Google Scholar

20. A. Sanyal, R. B. Mailliard, C. R. Rinaldo, D. Ratner, M. Ding, Y. Chen, J. M. Zerbato, N. S. Giacobbi, N. J. Venkatachari, B. K. Patterson, A. Chargin, N. Sluis-Cremer, P. Gupta, Novel assay reveals a large, inducible, replication-competent HIV-1 reservoir in resting $CD4^+$ T cells. *Nat. Med.* **23**, 885–889 (2017). CrossRef Google Scholar

21. N. T. Sebastian, T. D. Zaikos, V. Terry, F. Taschuk, L. A. McNamara, A. Onafuwa-Nuga, R. Yucha, R. A. J. Signer, J. Riddell IV., D. Bixby, N. Markowitz, S. J. Morrison, K. L. Collins, CD4 is expressed on a heterogeneous subset of hematopoietic progenitors, which persistently harbor CXCR4 and CCR5-tropic HIV proviral genomes in vivo. *PLOS Pathog.* **13**, e1006509 (2017). CrossRef Google Scholar

22. J. B. Dinoso, S. Y. Kim, A. M. Wiegand, S. E. Palmer, S. J. Gange, L. Cranmer, A. O'Shea, M. Callender, A. Spivak, T. Brennan, M. F. Kearney, M. A. Proschan, J. M. Mican, C. A. Rehm, J. M. Coffin, J. W. Mellors, R. F. Siliciano, F. Maldarelli, Treatment intensification does not reduce residual HIV-1 viremia in patients on highly active antiretroviral therapy. *Proc. Natl. Acad. Sci. U.S.A.* **106**, 9403–9408 (2009). Abstract/FREE Full Text Google Scholar

23. E. Eisele, R. F. Siliciano, Redefining the viral reservoirs that prevent HIV-1 eradication. *Immunity* **37**, 377–388 (2012). CrossRef PubMed Web of Science Google Scholar

24. P. J. Ballem, A. Belzberg, D. V. Devine, D. Lyster, B. Spruston, H. Chambers, P. Doubroff, K. Mikulash, Kinetic studies of the mechanism of thrombocytopenia in patients with human immunodeficiency virus infection. *N. Engl. J. Med.* **327**, 1779–1784 (1992). CrossRef PubMed Web of Science Google Scholar

25. J. E. Italiano Jr., J. Hartwig, Production and destruction of platelets, in *The Non-Thrombotic Role of Platelets in Health and Disease*, S. W. Kerrigan, Ed. (IntechOpen, 2015).

26. R. Grozovsky, S. Giannini, H. Falet, K. M. Hoffmeister, Molecular mechanisms regulating platelet clearance and thrombopoietin production. *ISBT Sci. Ser.* **10**, 309–316 (2015). Google Scholar

27. R. Grozovsky, K. M. Hoffmeister, H. Falet, Novel clearance mechanisms of platelets. *Curr. Opin. Hematol.* **17**, 585–589 (2010). CrossRef PubMed Google Scholar

28. R. D'Amico, Y. Yang, D. Mildvan, S. R. Evans, C. T. Schnizlein-Bick, R. Hafner, N. Webb, M. Basar, R. Zackin, M. A. Jacobson, Lower CD4+ T lymphocyte nadirs may indicate limited immune reconstitution in HIV-1 infected individuals on potent antiretroviral therapy: Analysis of immunophenotypic marker results of AACTG 5067. *J. Clin. Immunol.* **25**, 106–115 (2005). CrossRef PubMed Web of Science Google Scholar

29. C. F. Kelley, C. M. Kitchen, P. W. Hunt, B. Rodriguez, F. M. Hecht, M. Kitahata, H. M. Crane, J. Willig, M. Mugavero, M. Saag, J. N. Martin, S. G. Deeks, Incomplete peripheral CD4+ cell count restoration in HIV-infected patients receiving long-term antiretroviral treatment. *Clin. Infect. Dis.* **48**, 787–794 (2009). CrossRef PubMed Web of Science Google Scholar

30. V. Rodrigues, N. Ruffin, M. San-Roman, P. Benaroch, Myeloid cell interaction with HIV: A complex relationship. *Front. Immunol.* **8**, 1698 (2017). CrossRef Google Scholar

31. Y. Ganor, F. Real, A. Sennepin, C. A. Dutertre, L. Prevedel, L. Xu, D. Tudor, B. Charmeteau, A. Couedel-Courteille, S. Marion, A. R. Zenak, J. P. Jourdain, Z. Zhou, A. Schmitt, C. Capron, E. A. Eugenin, R. Cheynier, M. Revol, S. Cristofari, A. Hosmalin, M. Bomsel, HIV-1 reservoirs in urethral macrophages of patients under suppressive antiretroviral therapy. *Nat. Microbiol.* **4**, 633–644 (2019). Google Scholar

32. J. M. Orenstein, Replication of HIV-1 in vivo and in vitro. *Ultrastruct. Pathol.* **31**, 151–167 (2007). CrossRef PubMed Web of Science Google Scholar

35. G. Cenderello, A. De Maria, Discordant responses to cART in HIV-1 patients in the era of high potency antiretroviral drugs: Clinical evaluation, classification, management prospects. *Expert Rev. Anti-Infect. Ther.* **14**, 29–40 (2016). Google Scholar

36. S. G. Deeks, HIV infection, inflammation, immunosenescence, and aging. *Annu. Rev. Med.* **62**, 141–155 (2011). CrossRef PubMed Web of Science Google Scholar

37. W. Lu, V. Mehraj, K. Vyboh, W. Cao, T. Li, J. P. Routy, CD4:CD8 ratio as a frontier marker for clinical outcome, immune dysfunction and viral reservoir size in virologically suppressed HIV-positive patients. *J. Int. AIDS Soc.* **18**, 20052 (2015). CrossRef PubMed Google Scholar

38. M. M. Lederman, L. Calabrese, N. T. Funderburg, B. Clagett, K. Medvik, H. Bonilla, B. Gripshover, R. A. Salata, A. Taege, M. Lisgaris, G. A. McComsey, E. Kirchner, J. Baum, C. Shive, R. Asaad, R. C. Kalayjian, S. F. Sieg, B. Rodriguez, Immunologic failure despite suppressive antiretroviral therapy is related to activation and turnover of memory CD4 cells. *J. Infect. Dis.* **204**, 1217–1226 (2011). CrossRef PubMed Google Scholar

39. J. B. Honeycutt, W. O. Thayer, C. E. Baker, R. M. Ribeiro, S. M. Lada, Y. Cao, R. A. Cleary, M. G. Hudgens, D. D. Richman, J. V. Garcia, HIV persistence in tissue macrophages of humanized myeloid-only mice during antiretroviral therapy. *Nat. Med.* **23**, 638–643 (2017). CrossRef Google Scholar

40. G. R. Kaufmann, L. Perrin, G. Pantaleo, M. Opravil, H. Furrer, A. Telenti, B. Hirschel, B. Ledergerber, P. Vernazza, E. Bernasconi, M. Rickenbach, M. Egger, M. Battegy; Swiss HIV Cohort Study Group, CD4 T-lymphocyte recovery in individuals with advanced HIV-1 infection receiving potent antiretroviral therapy for 4 years: The Swiss HIV cohort study. *Arch. Intern. Med.* **163**, 2187–2195 (2003). CrossRef PubMed Web of Science Google Scholar

41. M. Marziali, W. De Santis, R. Carello, W. Leti, A. Esposito, A. Isgrò, C. Fimiani, M. C. Sirianni, I. Mezzaroma, F. Aiuti, T-cell homeostasis alteration in HIV-1 infected subjects with low CD4 T-cell count despite undetectable virus load during HAART. *AIDS* **20**, 2033–2041 (2006). CrossRef PubMed Web of Science Google Scholar

42. W. H. V. Carvalho-Silva, J. L. Andrade-Santos, F. O. Souto, A. V. C. Coelho, S. Crovella, R. L. Guimarães, Immunological recovery failure in cART-treated HIV-positive patients is associated with reduced thymic output and RTE CD4+ T cell death by pyroptosis. *J. Leukoc. Biol.* **107**, 85–94 (2020). Google Scholar

43. P. Harrison, I. Mackie, A. Mumford, C. Briggs, R. Liesner, M. Winter, S. Machin; British Committee for Standards in Haematology, Guidelines for the laboratory investigation of heritable disorders of platelet function. *Br. J. Haematol.* **155**, 30–44 (2011). CrossRef PubMed Google Scholar

44. Y. Kajikawa, T. Morihara, H. Sakamoto, K. Matsuda, Y. Oshima, A. Yoshida, M. Nagae, Y. Arai, M. Kawata, T. Kubo, Platelet-rich plasma enhances the initial mobilization of circulation-derived cells for tendon healing. *J. Cell. Physiol.* **215**, 837–845 (2008). CrossRef PubMed Web of Science Google Scholar

45. S. Amisten, A rapid and efficient platelet purification protocol for platelet gene expression studies. *Methods Mol. Biol.* **788**, 155–172 (2012). CrossRef PubMed Google Scholar

46. C. Palmer, M. Diehn, A. A. Alizadeh, P. O. Brown, Cell-type specific gene expression profiles of leukocytes in human peripheral blood. *BMC Genomics* **7**, 115 (2006). CrossRef PubMed Google Scholar

47. R. Arrigucci, Y. Bushkin, F. Radford, K. Lakehal, P. Vir, R. Pine, D. Martin, J. Sugarman, Y. Zhao, G. S. Yap, A. A. Lardizabal, S. Tyagi, M. L. Gennaro, FISH-flow, a protocol for the concurrent detection of mRNA and protein in single cells using fluorescence in situ hybridization and flow cytometry. *Nat. Protoc.* **12**, 1245–1260 (2017). Google Scholar

48. K. R. Gabriel, C. L. Odoroff, Biplots in biomedical research. *Stat. Med.* **9**, 469–485 (1990). PubMed Web of Science Google Scholar

49. K. Tenner-Racz, P. Rácz, M. Dietrich, P. Kern, Altered follicular dendritic cells and virus-like particles in AIDS and AIDS-related lymphadenopathy. *Lancet* **1**, 105–106 (1985). CrossRef PubMed Google Scholar

50. K. Tenner-Racz, P. Racz, M. Bofill, A. Schulz-Meyer, M. Dietrich, P. Kern, J. Weber, A. J. Pinching, F. Veronese-Dimarzo, M. Popovic, D. Klatzmann, J. C. Gluckman, G. Janossy, HTLV-III/LAV viral antigens in lymph nodes of homosexual men with persistent generalized lymphadenopathy and AIDS. *Am. J. Pathol.* **123**, 9–15 (1986). PubMed Web of Science Google Scholar

51. A. Le Tourneau, J. Audouin, J. Diebold, C. Marche, V. Tricottet, M. Reynes, LAV-like viral particles in lymph node germinal centers in patients with the persistent lymphadenopathy syndrome and the acquired immunodeficiency syndrome-related complex: An ultrastructural study of 30 cases. *Hum. Pathol.* **17**, 1047–1053 (1986). CrossRef PubMed Google Scholar

52. C. J. O'Hara, J. E. Groopman, M. Federman, The ultrastructural and immunohistochemical demonstration of viral particles in lymph nodes from human immunodeficiency virus-related and non-human immunodeficiency virus-related lymphadenopathy syndromes. *Hum. Pathol.* **19**, 545–549 (1988). CrossRef PubMed Google Scholar

53. A. Morner, A. Björndal, J. Albert, V. N. Kewalramani, D. R. Littman, R. Inoue, R. Thorstensson, E. M. Fenyö, E. Björling, Primary human immunodeficiency virus type 2 (HIV-2) isolates, like HIV-1 isolates, frequently use CCR5 but show promiscuity in coreceptor usage. *J. Virol.* **73**, 2343–2349 (1999). Abstract/FREE Full Text Google Scholar

54. A. M. Janas, L. Wu, HIV-1 interactions with cells: From viral binding to cell-cell transmission. *Curr. Protoc. Cell Biol.* **Chapter 26**, Unit 26.5 (2009). Google Scholar

55. M. K. Liszewski, J. J. Yu, U. O'Doherty, Detecting HIV-1 integration by repetitive-sampling Alu-gag PCR. *Methods* **47**, 254–260 (2009). CrossRef PubMed Web of Science Google Scholar

56. W. De Spiegelaere, E. Malatinkova, L. Lynch, F. Van Nieuwerburgh, P. Messiaen, U. O'Doherty, L. Vandekerckhove, Quantification of integrated HIV DNA by repetitive-sampling Alu-HIV PCR on the basis of poisson statistics. *Clin. Chem.* **60**, 886–895 (2014). Abstract/FREE Full Text Google Scholar

59. F. Real, A. Sennepin, Y. Ganor, A. Schmitt, M. Bomsel, Live imaging of HIV-1 transfer across T cell virological synapse to epithelial cells that promotes stromal macrophage infection. *Cell Rep.* **23**, 1794–1805 (2018). CrossRef Google Scholar

60. L. Prevedel, N. Ruel, P. Castellano, C. Smith, S. Malik, C. Villeux, M. Bomsel, S. Morgello, E. A. Eugenin, Identification, localization, and quantification of HIV reservoirs using microscopy. *Curr. Protoc. Cell Biol.* **82**, e64 (2019). Google Scholar

61. V. Henn, J. R. Slupsky, M. Gräfe, I. Anagnostopoulos, R. Förster, G. Müller-Berghaus, R. A. Kroczek, CD40 ligand on activated platelets triggers an inflammatory reaction of endothelial cells. *Nature* **391**, 591–594 (1998). CrossRef PubMed Web of Science Google Scholar

62. S. Raymond, N. Jeanne, F. Nicot, C. Lefebvre, R. Carcenac, L. Minier, J. Chiabrando, M. Cazabat, P. Delobel, J. Izopet, Long-term evolution of transmitted CXCR4-using HIV-1 under effective antiretroviral therapy. *AIDS* **33**, 1977–1985 (2019). Google Scholar

63. N. Jeanne, A. Saliou, R. Carcenac, C. Lefebvre, M. Dubois, M. Cazabat, F. Nicot, C. Loiseau, S. Raymond, J. Izopet, P. Delobel, Position-specific automated processing of V3 env ultra-deep pyrosequencing data for predicting HIV-1 tropism. *Sci. Rep.* **5**, 16944 (2015). Google Scholar

64. R. C. Edgar, MUSCLE: Multiple sequence alignment with high accuracy and high throughput. *Nucleic Acids Res.* **32**, 1792–1797 (2004). CrossRef PubMed Web of Science Google Scholar

65. S. Capella-Gutiérrez, J. M. Silla-Martínez, T. Gabaldón, trimAl: A tool for automated alignment trimming in large-scale phylogenetic analyses. *Bioinformatics* **25**, 1972–1973 (2009). CrossRef PubMed Web of Science Google Scholar

66. S. Guindon, O. Gascuel, A simple, fast, and accurate algorithm to estimate large phylogenies by maximum likelihood. *Syst. Biol.* **52**, 696–704 (2003). CrossRef PubMed Web of Science Google Scholar

67. D. Darriba, G. L. Taboada, R. Doallo, D. Posada, jModelTest 2: More models, new heuristics and parallel computing. *Nat. Methods* **9**, 772 (2012). CrossRef PubMed Google Scholar

68. ↵ I. Letunic, P. Bork, Interactive tree of life (iTOL) v4: Recent updates and new developments. *Nucleic Acids Res.* **47**, W256–W259 (2019). Google Scholar

Acknowledgments: We thank the HIV-infected individuals who participated in this study, V. Boeva from Institut Cochin for advice on multivariate analysis, and A. Schmitt for help with electron microscopy. **Funding:** This work was supported by Agence Nationale de Recherches sur le Sida et les Hépatites Virales (ANRS #AO2015-2-17046) and SIDACTION (#15CONV03) to M.B. F.R. is the recipient of a postdoctoral fellowship from SIDACTION and ANRS. L.X. and A.Z. received doctoral fellowships from the Chinese Science Council, and A.S. is an ANRS postdoctoral fellow. **Author contributions:** F.R., E.C.B., and M.B. conceived the experiments. C.C., S.G., E.R., and E.C.B. collected the patient samples and provided clinical information. F.R., C.C., and M.B. performed flow cytometry and confocal microscopy. F.R., G.S., and J.Z. performed reporter T cell assays. F.R., A.S., A.Z., and L.X. performed qPCR experiments. F.R., C.C., J.-M.M., and M.B. performed electron microscopy. F.R., R.A., M.L.G., and M.B. set up FISH and flow cytometry assays. F.R., M.B., E.E., and M.D. designed and performed in situ hybridization experiments on megakaryocytes and platelets in vitro. M.C., P.D., and J.I. performed deep sequencing and phylogenetic analyses of HIV *env* gene V3 segments. F.R., S.G., E.R., E.C.B., and M.B. performed retrospective and prospective analysis of the clinical status of HIV-infected individuals. F.R., E.C.B., and M.B. wrote the manuscript. **Competing interests:** The authors declare that they have no competing interests. **Data and materials availability:** All data associated with this study are in the paper or the Supplementary Materials. HIV *env* V3 sequences have been deposited in GenBank with accession numbers **MN453286**, **MN453287**, **MN453286 MN453288**, **MN453289**, **MN453290**, **MN453291**, **MN453292**, **MN453293**, **MN453294**, and **MN453295**.

View Abstract

Science Translational Medicine
Vol 12, Issue 535
18 March 2020

Table of Contents

RELATED CONTENT

Research Article
Abundant HIV-infected cells in blood and tissues are rapidly cleared upon ART initiation during acute HIV infection

Research Article
An open-label phase 1 clinical trial of the anti-$\alpha_4\beta_7$ monoclonal antibody vedolizumab in HIV-infected individuals

Research Article
Heterogeneous antiretroviral drug distribution and HIV/SHIV detection in the gut of three species

Research Article
Multispecific anti-HIV duoCAR-T cells display broad in vitro antiviral activity and potent in vivo elimination of HIV-infected cells in a humanized mouse model

Research Article
Single-cell transcriptional landscapes reveal HIV-1–driven aberrant host gene transcription as a potential therapeutic target

Reports
Structural basis for transcriptional start site control of HIV-1 RNA fate

In Depth
Long-acting drug acts like a short-term AIDS vaccine

Reports
Number of HIV-1 founder variants is determined by the recency of the source partner infection

Research Articles

Recapitulation of HIV-1 Env-antibody coevolution in macaques leading to neutralization breadth

SIMILAR ARTICLES IN:

- PubMed
- Google Scholar

CITED BY... +

CITING ARTICLES IN:

- Web of Science (10)

Vol 371, Issue 6525

Table of Contents

SCIENCE FOR POLICY: COVID-19

Coevolution of policy and science during the pandemic

PSYCHOLOGY

Play breeds better thinkers

SCI COMMUN

News at a glance

CORONAVIRUS

SARS-CoV-2 spillover events

WORKING LIFE

Breaking through language barriers

Get Our E-Alerts

Receive emails from *Science*. See full list

- [x] *Science Translational Medicine* TOC
- [x] *Science* Daily News
- [x] Weekly News Roundup
- [x] *Science* Editor's Choice
- [x] First Release Notification

United States

Email address*

- [ ] I also wish to receive emails from AAAS/*Science* and *Science* advertisers, including information on products, services, and special offers which may include but are not limited to news, career information, & upcoming events.

Sign up today

Required fields are indicated by an asterisk (*)

Science Translational Medicine ISSN 1946-6242.